Available online at www.sciencedirect.com
ScienceDirect
C. R. Mecanique 335 (2007) 323–329
COMPTES RENDUS MECANIQUE
http://france.elsevier.com/direct/CRAS2B/

Melting and solidification: processes and models/Processes and control of crystal growth

Controlling the growth interface shape in the growth of CdTe single crystals by the traveling heater method

Sadik Dost *, YongCai Liu

Crystal Growth Laboratory, University of Victoria, BC, Canada V8W 3P6

Available online 22 June 2007

Abstract

This article presents the results of a numerical simulation study carried out for controlling the growth interface shape in the THM (Traveling Heater Method) growth of CdTe single crystals. Applying different thermal boundary conditions and a crucible rotation, the optimum growth conditions for a desired interface shape were obtained. The simulation results show that by controlling the heat removal at the bottom of the crucible, a flatter (or slightly concave towards the crystal) growth interface can be maintained throughout the growth process. A crucible rotation rate of 5 rpm seems optimal for a favorable growth interface shape. ***To cite this article: S. Dost, Y.C. Liu, C. R. Mecanique 335 (2007).***

Résumé

Contrôle de l'interface lors de la croissance cristalline du CdTe par la méthode THM. Cet article présente les résultats de simulations numériques conduites afin d'examiner l'évolution et le contrôle de l'interface lors de la croissance cristalline du CdTe par la méthode THM. Des conditions de croissance optimales sont identifiées en effectuant des simulations pour une gamme de conditions thermiques aux frontières ainsi que pour différents taux de rotations de l'ampoule. Les résultats montrent qu'un contrôle judicieux du taux d'extraction de chaleur par la base de l'ampoule favorise une croissance en interface plane durant tout le processus. Un taux de rotation optimal de 5 rpm apparaît comme étant optimal pour le maintien d'une interface relativement plane. ***Pour citer cet article : S. Dost, Y.C. Liu, C. R. Mecanique 335 (2007).***

Keywords: Computation fluid mechanics; Crystal growth; Numerical analysis; Interface shapes

Mots-clés : Mécanique des fluides numérique ; Croissance cristalline ; Analyse numérique ; Interface

1. Introduction

Cadmium telluride (CdTe, and also CdZnTe) single crystals have been used for a variety of applications, such as optoelectronic modulators, prisms, gamma- and X-ray detectors, and substrates for far infrared HgCdTe photodetectors and radiation detectors. Such applications have led to an increasing interest in the crystal growth of CdTe and its related compounds (see for instance [1,2]).

* Corresponding author.
E-mail address: sdost@me.uvic.ca (S. Dost).

1631-0721/$ – see front matter
doi:10.1016/j.crme.2007.05.011

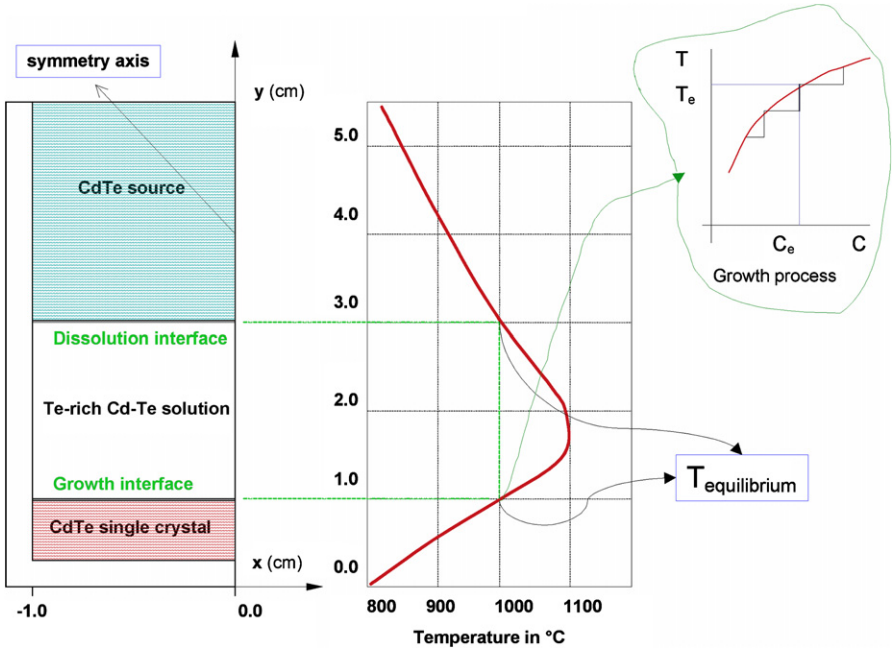

Fig. 1. Schematic view of the THM growth cell, and the applied temperature profile when the system is stationary.

Fig. 1. Aperçu d'une cellule de croissance THM et profil de température appliqué au système stationnaire.

The Traveling Heater Method (THM), a solution growth technique, has the potential for growing bulk binary and ternary crystals at relatively low temperatures. Related theoretical and modeling studies of the THM can be found in [3–8] (and references therein).

In THM, the control of the growth interface shape is very important. Generally a flat or slightly concave interface towards the solid is desirable, to prevent solvent inclusions and polycrystalline growth [8]. However, the control of the shape of the growth interface in the THM growth process is very difficult since the evolution of the growth interface is influenced by convection in the solution and also by the heat and mass transfer in the vicinity of the growth and dissolution interfaces. In order to investigate this issue, we have carried out a three dimensional numerical simulation study to determine the conditions for an optimum interface shape using various thermal boundary conditions and also by introducing a crucible rotation.

2. The model

2.1. Schematic view and governing equations

The schematic view of the simulation model for the THM growth system used in our laboratory and the applied furnace temperature profile and coordinate system are shown in Fig. 1. The THM growth is realized by the slow relative motion of the applied temperature profile, by moving either the heater or the growth ampoule. When the temperature profile moves upwards, the solution–source interface (dissolution interface) hits the hotter section of the temperature profile and dissolves the source material. This dissolution provides constantly the needed material to the liquid solution. With the movement of the temperature profile, at the same time, the seed–solution interface (growth interface) hits the cooler section of the temperature profile, and the supersaturated solution in the vicinity of the growth interface solidifies on the seed crystals.

In the model we assume that the liquid solution (Te-rich dilute binary mixture) is an incompressible, Newtonian viscous liquid, and the well-known Boussinesq approximation holds. The flow in the liquid solution is laminar. The solid phase, which represents the seed and feed crystals and the crucible wall, is a heat conducting rigid material.

The governing equations of continuity, momentum, mass transport, and heat transfer are included in the liquid phase:

$$\frac{1}{r}\frac{\partial}{\partial r}(ru)+\frac{1}{r}\frac{\partial v}{\partial \varphi}+\frac{\partial w}{\partial z}=0 \tag{1}$$

$$\frac{\partial u}{\partial t}+u\frac{\partial u}{\partial r}+\frac{v}{r}\frac{\partial u}{\partial \varphi}+w\frac{\partial u}{\partial z}-\frac{v^2}{r}=\nu\left[\frac{1}{r}\frac{\partial}{\partial r}\left(r\frac{\partial u}{\partial r}\right)+\frac{1}{r^2}\frac{\partial^2 u}{\partial \varphi^2}+\frac{\partial^2 u}{\partial z^2}-\frac{u}{r^2}-\frac{2}{r^2}\frac{\partial v}{\partial \varphi}\right]-\frac{1}{\rho}\frac{\partial p}{\partial r} \tag{2}$$

$$\frac{\partial v}{\partial t}+u\frac{\partial v}{\partial r}+\frac{v}{r}\frac{\partial v}{\partial \varphi}+w\frac{\partial v}{\partial z}+\frac{uv}{r}=\nu\left[\frac{1}{r}\frac{\partial}{\partial r}\left(r\frac{\partial v}{\partial r}\right)+\frac{1}{r^2}\frac{\partial^2 v}{\partial \varphi^2}+\frac{\partial^2 v}{\partial z^2}-\frac{v}{r^2}+\frac{2}{r^2}\frac{\partial v}{\partial \varphi}\right]-\frac{1}{\rho r}\frac{\partial p}{\partial \varphi} \tag{3}$$

$$\frac{\partial w}{\partial t}+u\frac{\partial w}{\partial r}+\frac{v}{r}\frac{\partial w}{\partial \varphi}+w\frac{\partial w}{\partial z}=\nu\left[\frac{1}{r}\frac{\partial}{\partial r}\left(r\frac{\partial w}{\partial r}\right)+\frac{1}{r^2}\frac{\partial^2 w}{\partial \varphi^2}+\frac{\partial^2 w}{\partial z^2}-\frac{1}{\rho}\frac{\partial p}{\partial z}\right] - g\beta_t(T-T_0)+g\beta_c(C-C_0) \tag{4}$$

$$\frac{\partial C}{\partial t}+u\frac{\partial C}{\partial r}+\frac{v}{r}\frac{\partial C}{\partial \varphi}+w\frac{\partial C}{\partial z}=D\left[\frac{1}{r}\frac{\partial}{\partial r}\left(r\frac{\partial C}{\partial r}\right)+\frac{1}{r^2}\frac{\partial^2 C}{\partial \varphi^2}+\frac{\partial^2 C}{\partial z^2}\right] \tag{5}$$

$$\frac{\partial T}{\partial t}+u\frac{\partial T}{\partial r}+\frac{v}{r}\frac{\partial T}{\partial \varphi}+w\frac{\partial T}{\partial z}=\frac{k}{\rho c_p}\left[\frac{1}{r}\frac{\partial}{\partial r}\left(r\frac{\partial T}{\partial r}\right)+\frac{1}{r^2}\frac{\partial^2 T}{\partial \varphi^2}+\frac{\partial^2 T}{\partial z^2}\right] \tag{6}$$

where u, v and w are the velocity components in the radial (r), circumferential (φ) and vertical (z) directions, respectively. ν, D, and β_t and β_c represent, respectively, the kinematic viscosity, the diffusion coefficient of CdTe in the Te-rich solution, the expansion and solutal expansion coefficients. p, T, and C are the pressure, temperature, and solute (CdTe) concentration in the Te-rich solvent, respectively. ρ, k_l, and c_p denote respectively the density, thermal conductivity and specific heat of the solution. T_o and C_o are the reference temperature and concentration, respectively, and g is the gravitational constant.

Since we consider a binary system (CdTe) in this study, the only governing equation in the solid phase is the energy balance that takes the following form:

$$\frac{\partial T}{\partial t}=\frac{k_s}{\rho_s c_{p,s}}\left[\frac{1}{r}\frac{\partial}{\partial r}\left(r\frac{\partial T}{\partial r}\right)+\frac{1}{r^2}\frac{\partial^2 T}{\partial \varphi^2}+\frac{\partial^2 T}{\partial z^2}\right] \tag{7}$$

where k_s, ρ_s, and $c_{p,s}$ represent respectively the thermal conductivity, density, and specific heat of the solid phase.

2.2. Boundary and interface conditions

In the liquid phase we assume at the vertical wall

$$u=0,\qquad v=2\pi\omega r,\qquad w=0,\qquad \frac{\partial C}{\partial r}=0 \tag{8}$$

where ω is the angular rotation of the ampoule. At the growth and dissolution interfaces, we take

$$u=0,\qquad v=0,\qquad w=0,\qquad T=T_m(C),\qquad -D\frac{\partial C}{\partial n}=(1-C)V_g(\mathbf{n}\cdot\mathbf{e}_z)$$
$$k\frac{\partial T}{\partial n}\bigg|_l-k\frac{\partial T}{\partial n}\bigg|_s=\rho_s\Delta H V_g(\mathbf{n}\cdot\mathbf{e}_z) \tag{9}$$

where $T_m(C)$ is the equilibrium solidification temperature at the growth interface and dissolution interface which is a function of solute concentration, V_g is the traveling rate of furnace temperature, ΔH is the latent heat, and $\mathbf{n}$ and $\mathbf{e}_z$ are the unit vectors in the normal direction to the interface and along the vertical direction, respectively. Since the flux conditions for the concentration field are used in all boundaries, an integrability condition [5] is needed to ensure a unique solution:

$$\int_V C\,\mathrm{d}V=V_1-V_0 \tag{10}$$

where V_1 is the volume of the solution region and V_0 the initial solvent volume. Eq. (10) is the overall mass conservation equation by assuming zero solubility of solvent in the solid phases so that the solute (CdTe) concentration is 1 in the source and crystal. This assumption is also a prerequisite for the concentration boundary condition given in Eq. (9).

The phase diagram relation is represented by

$$C = a\mathrm{e}^{(b-c/T)} \tag{11}$$

with temperature T given in Kelvin (K). The interfacial heat balance (the last boundary condition in Eq. (9)) is used to locate the shape and position of growth and dissolution interfaces, which is different from the treatment in [7] where the isotherm condition was directly applied at the interfaces.

The thermal boundary condition surrounding the outer ampoule (vertical wall, top surface, and bottom surface) is given as:

$$-k_s \frac{\partial T}{\partial n} = h\big[T - T_f(z,t)\big] \tag{12}$$

where h is the overall heat transfer coefficient that combines the effect of heat conduction and radiation, and is estimated based on the real measurement of the temperature difference between the furnace temperature and the temperature at the inner wall of the ampoule when it is empty. $T_f(z,t)$ represents the furnace temperature along the ampoule vertical wall, or at the top surface position, or at the bottom surface position.

The thermal boundary condition needs to be modified when we consider heat removal at the bottom of the ampoule. In our experimental set up, the cooling area is a circle concentric with the bottom surface of the ampoule and with a radius of 7 mm. The boundary condition for this area is given by

$$-k_s \frac{\partial T}{\partial n} = h_b h\big[T - T_f(z,t) - T_b\big] \tag{13}$$

where h_b and T_b are the constants that determine the degree of heat removal. We considered two cases: small heat removal $h_b = 1$ and $T_b = 110$, and large heat removal $h_b = 50$ and $T_b = 110$.

The initial conditions are taken as the equilibrium state of the system when the furnace thermal profile is stationary. The growth and dissolution interface shapes, and the positions of the interfaces are obtained iteratively by adjusting the interfaces to fit to the isotherm contours at their equilibrium temperatures. Therefore, the selection of the furnace temperature profile is very important for obtaining the desired interface shapes at the desired equilibrium temperatures. After a certain time, the temperature, concentration, and velocity fields become steady, which are taken as the initial values in the computations.

The flow, concentration, and temperature fields computed for a stationary system (at the beginning of the growth process) (which are not given here for reasons of space, see [7]) have shown that the growth interface has a double-humped shape. A slight asymmetry was observed in the concentration field. These transport structure values are used in our computations as the initial conditions.

The commercial CFX software from AEA Technology is used to solve the model equations. Several user-defined Fortran subroutines were developed and used to deal with the moving grid and complex temperature boundary conditions. The flow is treated as laminar [7]. The derivatives with respect to time are calculated by the backward finite difference algorithm. The hybrid-differencing scheme, which is a modification of the upwind-differencing method and is the default setting in CFX, is used for the discretization of the convective terms. Higher-order differencing schemes are found to be not robust for our problem. The computation mesh in the liquid is $60 \times 80 \times 80$ in the r-, φ-, and z-directions, respectively, which is demonstrated to be sufficient for an accurate and stable solution.

3. Simulation results and discussion

The physical properties and system parameters used in our simulations are given in Table 1. In the table, the liquid represents the Te-rich solution and the solid stands for the grown CdTe crystal and the CdTe feed.

Fig. 2 presents the time evolution of the growth interface. The simulation results show that as the growth interface evolves the thermal field of the system changes and the growth interface becomes flatter. This implies that by changing the thermal characteristics of the system we can make the growth interface slightly concave (towards the crystal), starting almost at the beginning of the growth process. We note that the interface shape at the beginning of the growth is almost the same as that given in [7], indicating that the simple isotherm treatment used at the growth interface in [7] led to sufficiently accurate predictions. This is because the growth velocity in the THM is very small; consequently we observe small concentration changes in the solution making the effect of the constitutional supercooling negligible [5].

Table 1
Physical properties and operating parameters of the CdTe THM growth system

Tableau 1
Propriétés physiques et paramètres opératoires du système de croissance de CdTe par la méthode THM

Parameter	Symbol	Values
Density of liquid	ρ	5.62 g/cm^3
Density of solid	ρ_s	5.68 g/cm^3
Density of silica	ρ_a	2.20 g/cm^3
Thermal conductivity of liquid	K	0.057 W/(cm K)
Thermal conductivity of solid	k_s	0.038 W/(cm K)
Thermal conductivity of silica	k_a	0.031 W/(cm K)
Specific heat of liquid	Cp	0.372 J/(g K)
Specific heat of solid	Cp_s	0.16 J/(g K)
Specific heat of silica	Cp_a	0.77 J/(g K)
Viscosity of liquid	μ	0.008992 g/(cm s)
Electrical conductivity of liquid	σ_E	2000.0 1/(Ω cm)
Thermal expansion coefficient	β_T	8.0×10^{-5} 1/K
Solute expansion coefficient	β_C	0.056
Diffusion coefficient of CdTe at Te solution	D	4.2×10^{-5} cm^2/s
Latent heat	ΔH	209.0 J/g
Furnace temperature traveling rate	V_g	0.2 cm/day
Crucible inner radius	R	1.3 cm
Crucible thickness		0.2 cm
Initial solution height	L	2.3 cm
Initial substrate thickness		0.7 cm
Initial source thickness		3.0 cm
Phase diagram coefficient	a	0.209
Phase diagram coefficient	b	8.2
Phase diagram coefficient	c	8607.29

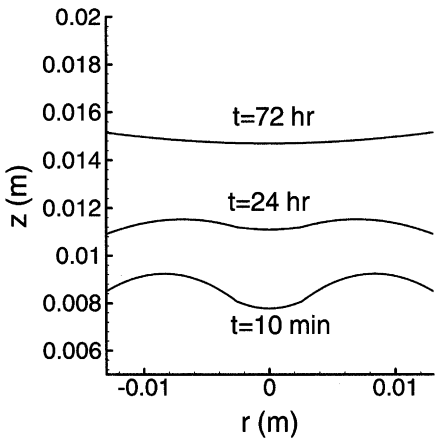

Fig. 2. The computed time evolution of the growth interface.
Fig. 2. Évolution de l'interface de croissance.

As mentioned earlier, a flat (or slightly concave interface) is desirable. In order to achieve this objective, we examined two options. The first one is to change the heat transfer conditions at the bottom surface of the ampoule (as done in experiments). The computed interface shapes and thermal fields under such thermal conditions are presented in Fig. 3. As can be seen, with the removal of more heat at the bottom of the ampoule, the shape of the isotherm lines near the growth interface change. Indeed, by controlling the heat removal at the bottom, the growth interface could be made flatter or even slightly convex to the solid. As the growth proceeds and the grown crystal gets thicker, the effect of the heat removal would become weaker unless the thermal conditions are adjusted. However, we know from

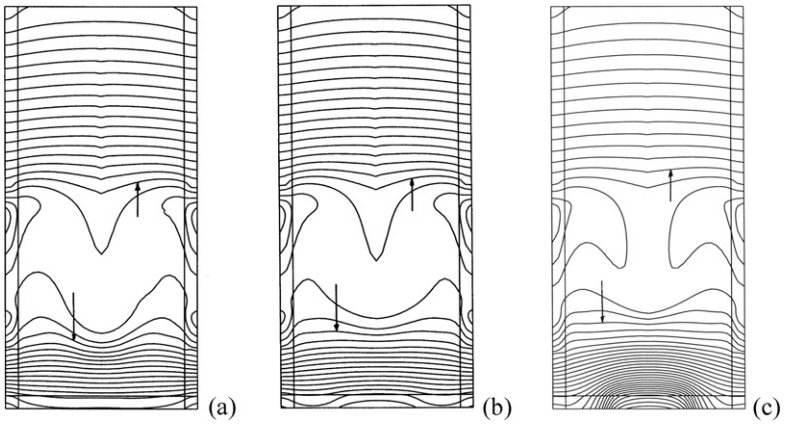

Fig. 3. The evolution of the thermal field (at $t = 10$ min growth time): (a) no heat removal; (b) small heat removal ($h_b = 1$ and $T_b = 110$ in Eq. (14)); (c) large heat removal ($h_b = 50$ and $T_b = 110$ in Eq. (14)). Contour spacing is $\Delta T = 10$ K, and the maximum and minimum temperatures are: (a) $T_{max} = 1041$ K and $T_{min} = 859$ K; (b) $T_{max} = 1041$ K and $T_{min} = 838$ K; and (c) $T_{max} = 1041$ K and $T_{min} = 750$ K.

Fig. 3. Évolution des champs thermiques (à $t = 10$ min de croissance) : (a) sans extraction de chaleur ; (b) faible extraction ($h_b = 1$ et $T_b = 110$ dans Eq. (14)) ; (c) extraction importante ($h_b = 50$ et $T_b = 110$). L'espacement des contours est de $\Delta T = 10$ K, les températures extrêmes sont : (a) $T_{max} = 1041$ K et $T_{min} = 859$ K ; (b) $T_{max} = 1041$ K et $T_{min} = 838$ K ; et (c) $T_{max} = 1041$ K et $T_{min} = 750$ K.

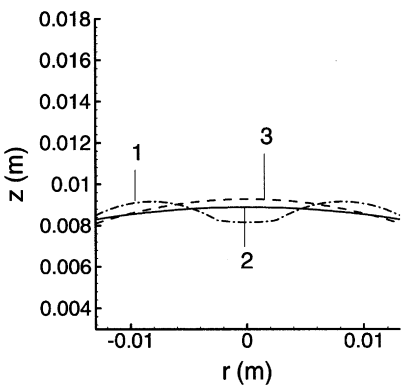

Fig. 4. Change of growth interface shape under various ampoule rotation rates: (1) at $\omega = 3$ rpm, (2) at $\omega = 5$ rpm, and (3) $\omega = 7$ rpm.

Fig. 4. Influence de la rotation de l'ampoule sur l'interface de croissance : (1) pour $\omega = 3$ rpm, (2) pour $\omega = 5$ rpm, et (3) $\omega = 7$ rpm.

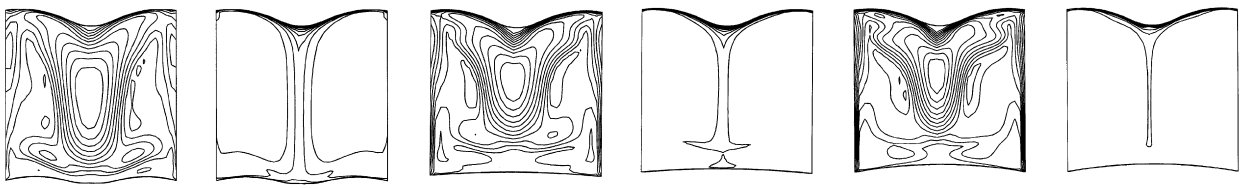

Fig. 5. The computed flow (left column) and concentration (right column) fields in the solution at: (a) $\omega = 3$ rpm; (b) $\omega = 5$ rpm; and (c) $\omega = 7$ rpm. In (a) the maximum and minimum flow strengths are $U_{max} = 0.0119$ m/s and $U_{min} = 0.0$ m/s, and the maximum and minimum concentrations are $C_{max} = 0.1286$ and $C_{min} = 0.1199$. In (b) $U_{max} = 0.0117$ m/s and $U_{min} = 0.0$ m/s, and $C_{max} = 0.1298$ and $C_{min} = 0.1219$. In (c) $U_{max} = 0.0126$ m/s and $U_{min} = 0.0$ m/s, and $C_{max} = 0.1303$ and $C_{min} = 0.1222$. Contour spacing is 0.001 m/s for the flow field and 0.001 for the concentration field.

Fig. 5. Champ dynamique (gauche) et de concentration (droite) pour : (a) $\omega = 3$ rpm ; (b) $\omega = 5$ rpm ; et (c) $\omega = 7$ rpm. (a) $U_{max} = 0{,}0119$ m/s et $U_{min} = 0{,}0$ m/s ; $C_{max} = 0{,}1286$ et $C_{min} = 0{,}1199$. (b) $U_{max} = 0{,}0117$ m/s et $U_{min} = 0{,}0$ m/s ; $C_{max} = 0{,}1298$ et $C_{min} = 0{,}1219$. (c) $U_{max} = 0{,}0126$ m/s et $U_{min} = 0{,}0$ m/s ; $C_{max} = 0{,}1303$ et $C_{min} = 0{,}1222$. L'espacement des contours est de 0,001.

the simulations in the absence of such a heat removal (Fig. 2) that the growth interface becomes flatter as the growth proceeds. Therefore, by controlling the heat removal at the bottom of the crucible, the desired growth interface shape can be maintained throughout the growth process.

As a second option, we also considered the rotation of the ampoule [8]. Fig. 4 gives the effect of a crucible rotation on the growth interface shape. An optimum growth interface was obtained under the rotation rate of 5 rpm, which agrees with the results of the two-dimensional simulations of [8].

The computed flow and concentration fields under three rotation rates are shown in Fig. 5. With an increase in the rotation rate, the flow field gets stronger near the vertical wall (see the left column of Fig. 5). The concentration field becomes more uniform everywhere in the solution except in the region near the dissolution interface, which could be beneficial for growing crystals with low point defects, but might be not favorable at higher growth rates due to the shallow concentration gradient near the growth interface which may lead to solvent inclusions in the grown crystal.

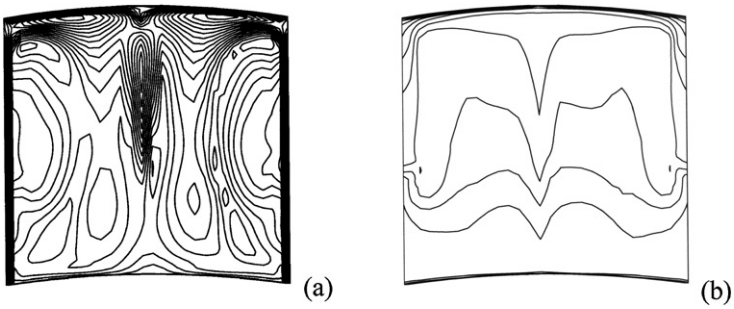

Fig. 6. The computed flow (a) and concentration (b) fields in the solution at $\omega = 15$ rpm. In (a) $U_{\max} = 0.0198$ m/s and $U_{\min} = 0.0$ m/s, with contour spacing 0.001 m/s; and in (b) $C_{\max} = 0.1271$ and $C_{\min} = 0.1209$, with contour spacing 0.001. Here $U = \sqrt{u^2 + v^2 + w^2}$.

Fig. 6. Champs simulés (a) dynamique et (b) de concentration pour $\omega = 15$ rpm. (a) $U_{\max} = 0{,}0198$ m/s et $U_{\min} = 0{,}0$ m/s. (b) $C_{\max} = 0{,}1271$ et $C_{\min} = 0{,}1209$. L'espacement des contours est de 0,001 (unité).

In order to make the study more complete, we also computed the thermal and concentration fields under a very high rotation rate: 15 rpm. In this case, the tangential flow velocity component near the vertical wall of the crucible is nearly twice that without rotation (Fig. 6). Flow instability may also occur since the flow structures become clearly asymmetric. The concentration field in the solution exhibit layer-like distributions at the whole region which reflects the domination of the circumferential flow.

4. Conclusions

The numerical simulations carried out for the THM growth of CdTe under various thermal and crucible rotation conditions showed that by controlling the heat removal at the bottom of the crucible, a flatter (or slight convex) growth interface can be maintained throughout the growth process. A crucible rotation rate of 5 rpm seems optimal for a favorable growth interface shape.

Acknowledgements

The financial support received from the Natural Sciences and Engineering Research Council of Canada (NSWRC) and Canada Research Chairs (CRC) Program is gratefully acknowledged.

References

[1] K. Sato, Y. Seki, Y. Matsuda, O. Oda, Recent developments in II–VI substrates, J. Crystal Growth 197 (1999) 413–422.
[2] P. Rudolph, M. Muhlberg, Basic problems of vertical Bridgman growth of CdTe, Mater. Sci. Eng. B 16 (1993) 8–16.
[3] R.A. Meric, S. Dost, B. Lent, R.F. Redden, A finite element model for the growth of ternary alloy GaInSb by the travelling heater method, Int. J. Appl. Electromagnet. Mech. 10 (1999) 505–526.
[4] X. Ye, B. Tabarrok, D. Walsh, The influence of the thermosolutal convection on CdTe growth by the traveling heater method, J. Crystal Growth 169 (1996) 704–714.
[5] C.W. Lan, O.T. Yang, A computational simulation of crystal growth by the traveling-solvent method (TSM): pseudo-steady-state calculations, Model. Simul. Mater. Sci. Eng. 3 (1995) 71–92.
[6] C.K. Ghaddar, C.K. Lee, S. Motakef, D.C. Gillies, Numerical simulation of THM growth of CdTe in presence of rotating magnetic fields (RMF), J. Crystal Growth 205 (1999) 97–111.
[7] Y.C. Liu, S. Dost, B. Lent, R.F. Redden, A three-dimensional numerical simulation model for the growth of CdTe single crystals by the traveling heater method under magnetic field, J. Crystal Growth 254 (2003) 285–297.
[8] Y. Okano, S. Nishino, S. Ohkubo, S. Dost, Numerical study of transport phenomena in the THM growth of compound semiconductor crystal, J. Crystal Growth 237–239 (2002) 1779–1784.